


## Synthesis and X-ray diffraction data of dichloro-dioxido-(4,4'-dimethyl-2,2'-bipyridyl) molybdenum (VI)

Jose L. Pinto,<sup>1</sup> Hernando Camargo,<sup>1</sup> and Nelson J. Castellanos <sup>2,a)</sup>

<sup>1</sup>Grupo de Investigación de Materiales de Interés Geológico y Geotécnico, Dirección de Laboratorios, Servicio Geológico Colombiano SGC, Diagonal 53 No. 34-53, Bogotá, Colombia

<sup>2</sup>Laboratorio de Diseño y Reactividad de Estructuras Sólidas (Lab-DRES, 125), Departamento de Química, Facultad de Ciencias, Universidad Nacional de Colombia, Carrera 30 No. 45-03, Bogotá 111321, Colombia

(Received 3 May 2022; accepted 16 December 2022)

The dichloro-dioxide-(4,4'-dimethyl-2,2'-bipyridyl)-molybdenum (VI) complex was prepared from molybdenum(VI)-dichloride-dioxide and 4,4'-dimethyl-2,2'-bipyridyl in CH<sub>2</sub>Cl<sub>2</sub> obtaining a clear green solution. The molybdenum complex was precipitated using ethyl ether, separated by filtration and the light green solid washed with ethyl ether. The XRPD pattern for the new compound showed that the crystalline compound belongs to the monoclinic space group *P2<sub>1</sub>/n* (No.14) with refined unit-cell parameters *a* = 12.0225(8) Å, *b* = 10.3812(9) Å, *c* = 11.7823(9) Å,  $\beta$  = 103.180(9)°, unit-cell volume *V* = 1431.79 Å<sup>3</sup>, and *Z* = 4.

© The Author(s), 2023. Published by Cambridge University Press on behalf of International Centre for Diffraction Data.

[doi:10.1017/S0885715623000040]

Key words: dioxomolybdenum (VI) complex, X-ray powder diffraction, biomimetic compounds

### I. INTRODUCTION

Molybdenum is an essential element in all forms of life (Schoepp-Cothenet et al., 2012; Kapp, 2014), and is mainly associated with enzymes that catalyze the oxidative process of a wide range of aldehydes and aromatic heterocycles, and oxygen atom transfer processes (OAT) in nature using the molecular oxygen (O<sub>2</sub>) as an oxidizing agent (Hille et al., 2011; Castellanos, 2014). These natural systems, known as molybdenum-enzymes, are the source of inspiration to synthesize different complexes called “biomimetics” that have allowed an advance in the understanding of the molecular oxygen activation mechanisms (Dupé et al., 2015; Heinze, 2015). Adapting these natural systems into analogous bio-inspired complexes, several structures of Mo<sup>VI</sup>O<sub>2</sub> with a variety of ligands have been synthesized and evaluated in OAT processes for substrates such as alkanes, alkenes, and phosphines (Bakhtchadjian et al., 2011; Kück et al., 2016). Recently, the photocatalytic activity of some dioxo-molybdenum complexes supported on different supports as metal-organic framework (MOF) or inorganic oxides as TiO<sub>2</sub> or SiO<sub>2</sub> were assessed in the selective epoxidation of terpenes as  $\alpha$ - and  $\beta$ -pinene or limonene, using molecular O<sub>2</sub> as the primary oxidizing agent (Castellanos et al., 2012, 2013; Martínez et al., 2018, 2020, 2021). In all cases, the epoxide was formed as the sole product and intermediate peroxy-molybdenum species were identified in the reoxidation process using infrared and EPR spectroscopy (Castellanos et al., 2021; Martínez

et al., 2022). In this work, we report the synthesis, molecular characterization (FTIR, NMR), and X-ray powder diffraction data of the dichloro-dioxido-(4,4'-dimethyl-2,2'-bipyridyl)-molybdenum (VI) complex as a biomimetic active center of molybdenum-enzymes.

### II. EXPERIMENTAL

All chemicals, including 4,4'-dimethyl-2,2'-bipyridine and MoO<sub>2</sub>Cl<sub>2</sub> were purchased from Sigma-Aldrich and used without further purification. Commercial grade solvents were dried and deoxygenated by refluxing for at least 12 h over appropriate drying agents under argon atmosphere and were freshly distilled prior to use. IR (KBr) were recorded with a Perkin-Elmer 1720XFT and <sup>1</sup>H and <sup>13</sup>C NMR were performed with Bruker Avance 400 spectrometer. The CHN elemental analysis was performed on a Thermo Scientific Flash 2000 CHNS/O analyzer equipped with a TCD detector. Molybdenum elemental analysis was carried out with an atomic absorption spectrophotometer Thermo S4. The samples were analyzed after acid digestion with previous calcination in a muffle furnace at 500 °C for 5 h.

#### A. Synthesis of dichloro-dioxo-(4,4'-dimethyl-2,2'-bipyridine)-molybdenum (VI)

A solution of dichloromethane (10 ml) containing 0.200 g (1.0 mmol) of MoO<sub>2</sub>Cl<sub>2</sub> was slowly added to 0.184 g (1.0 mmol) of the 4,4'-dimethyl-2,2'-bipyridine ligand dissolved in dichloromethane (15 ml) under a nitrogen atmosphere (Figure 1). The reaction was stirred for 12 h at room temperature protected from light. The reaction mixture was

<sup>a)</sup>Author to whom correspondence should be addressed. Electronic mail: njcastellanosm@unal.edu.co



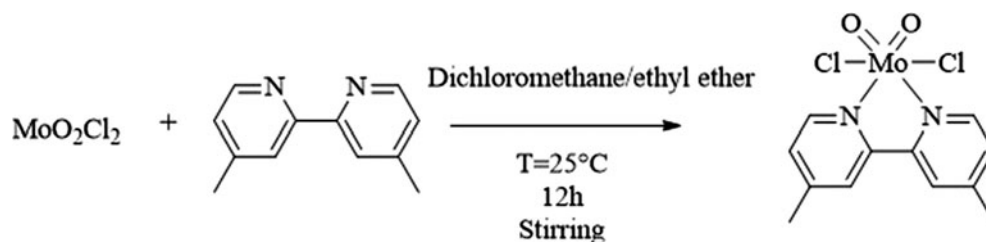


Figure 1. Synthesis of dichloro-dioxido-(4,4'-dimethyl-2,2'-bipyridyl)-molybdenum (VI) complex.

mixed with 15 ml of ethyl ether and the resulting solid was filtered and washed three times with 20 ml of ethyl ether to obtain a light green solid. (0.220 g; %R = 57.2) IR ( $\text{cm}^{-1}$ ) KBr: 3074 (=CH), 2988 (CH), 1616 (C=C), 1423 (C=C), 935 ( $\text{Mo}=\text{O}_{\text{asym}}$ ), 907 ( $\text{Mo}=\text{O}_{\text{sym}}$ ).  $^1\text{H}$  NMR (400 MHz,  $\text{CDCl}_3$ )  $\delta$  9.43 (d,  $J$  = 5.5 Hz, 2H), 8.05 (s, 2H), 7.53 (d,  $J$  = 7.8 Hz, 2H), 2.62 (s, 6H). Elemental analysis calculated for  $\text{C}_{12}\text{H}_{12}\text{Cl}_2\text{MoN}_2\text{O}_2$  (383.1): C 37.62, H 3.16, N 7.31. Found: C 37.81, H 2.98, N 6.98. Molybdenum elemental calculated: 25.1%, obtained: 27.0%.

### B. Data collection

X-ray powder diffraction (XRPD) of the dichloro-dioxido-(4,4'-dimethyl-2,2'-bipyridyl)-molybdenum (VI) complex was carried out at 298 K using an X'Pert Pro MPD PANalytical equipment with Cu anode ( $\text{CuK}\alpha$  radiation,  $\lambda$  = 1.5418 Å) and Bragg–Brentano geometry using a nickel filter and with a high-speed solid-state detector for data acquisition PIXcel. A receiving slit (RS) of 0.6 mm and primary and secondary soller slits (SS) of  $2.5^\circ$  were used. The diffraction data

were collected over the range from  $5.00$  to  $-80.00^\circ 2\theta$  with a step size of  $0.0263^\circ 2\theta$  and counting time of 97.920 s with a No. of points of 2856.

### III. RESULTS AND DISCUSSION

The synthesis and single-crystal structure of the dichloro-dioxido-(4,4'-dimethyl-2,2'-bipyridyl)-molybdenum (VI) complex were initially reported at room temperature using molybdenum acetate as precursor and collected X-ray data at 173 K (Baird et al., 1996) obtaining a monoclinic unit cell with  $a$  = 11.7556 (2),  $b$  = 10.369 (62),  $c$  = 11.956 (2) Å,  $\alpha$  =  $90^\circ$ ,  $\beta$  =  $103.57 (2)^\circ$ ,  $\gamma$  =  $90^\circ$ ,  $V$  = 1415.5 (5) Å<sup>3</sup>, and a space group  $P2_1/n$  (No.14). In this study, reaction at room temperature (298 K) using  $\text{MoO}_2\text{Cl}_2$  as molybdenum source, yields the title compound which was confirmed by their elemental and spectroscopic analysis. The powder diffraction pattern (Figure 2) was indexed on a monoclinic unit cell with least squares fit lattice parameters  $a$  = 11.9914 (4),  $b$  = 10.3662 (4),  $c$  = 11.7556 (4) Å,  $\beta$  =  $103.126 (3)^\circ$ ,  $V$  = 1423.11 Å<sup>3</sup> using DICVOL04 program (Boultif and Louër, 2004) and PreDICT

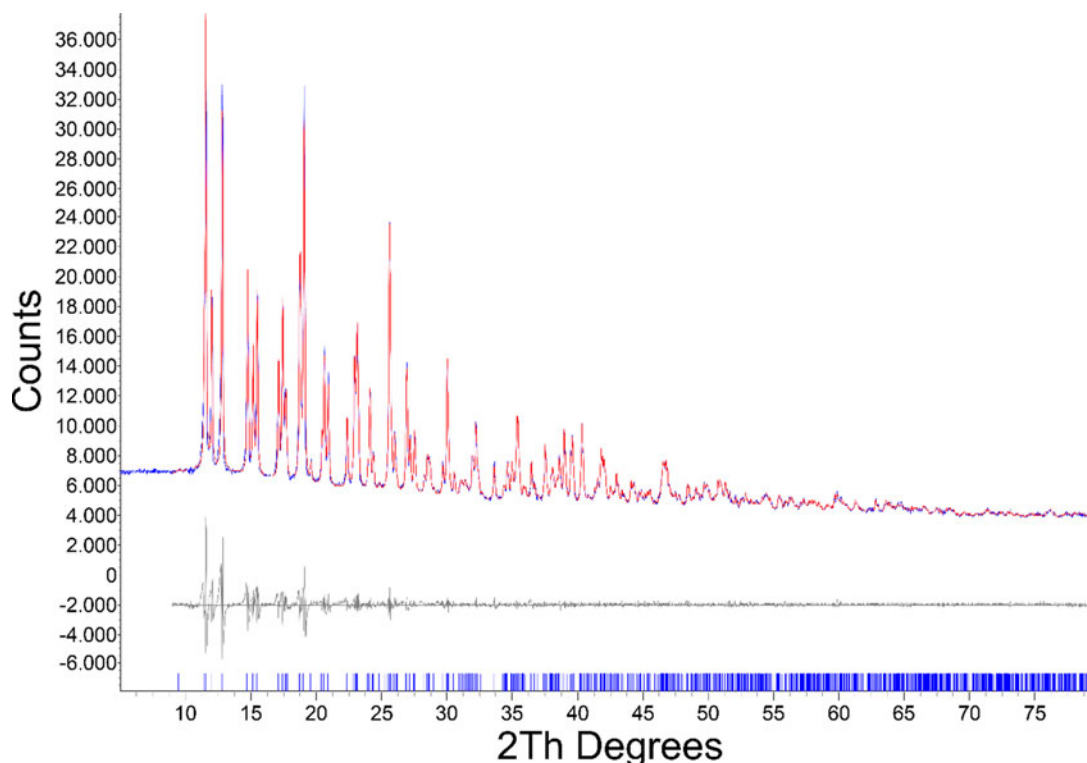


Figure 2. X-ray powder diffraction pattern of the title compound using  $\text{CuK}\alpha$  radiation (blue solid line) and the refined pattern of the compound (red solid line).

TABLE I. X-ray powder diffraction data for dichloro-dioxide-(4,4'-dimethyl-2,2'-bipyridyl)-molybdenum (VI) complex.

<i>h</i>	<i>k</i>	<i>l</i>	<i>d</i> <sub>obs</sub> (Å)	<i>d</i> <sub>cal</sub> (Å)	$\Delta d$	$2\theta_{\text{obs}}$ (°)	$2\theta_{\text{cal}}$ (°)	$\Delta 2\theta$	<i>I</i> / <i>I</i> <sub>o</sub>
0	0	1	11.4625	11.4523	0.0102	7.7064	7.7132	-0.0068	36.3
0	1	1	7.6560	7.6789	-0.0229	11.5487	11.5142	0.0345	100.0
1	0	1	7.3554	7.3715	-0.0161	12.0225	11.9960	0.0264	38.2
1	1	-1	6.9031	6.9234	-0.0203	12.8134	12.7756	0.0378	78.2
1	1	1	5.9972	6.0044	-0.0072	14.7589	14.7412	0.0177	44.7
2	0	0	5.8287	5.8358	-0.0071	15.1881	15.1695	0.0186	28.7
0	0	2	5.7133	5.7262	-0.0128	15.4966	15.4617	0.0349	41.1
0	2	0	5.1728	5.1752	-0.0023	17.1274	17.1196	0.0078	25.1
2	1	0	5.0807	5.0834	-0.0027	17.4404	17.4309	0.0095	39.0
0	1	2	5.0115	5.0105	0.0010	17.6832	17.6867	-0.0035	21.0
1	2	0	4.7252	4.7310	-0.0058	18.7640	18.7409	0.0231	53.4
1	0	2		4.7291	-0.0039		18.7483	0.0157	
0	2	1		4.7160	0.0092		18.8009	-0.0369	
2	0	-2	4.6469	4.6569	-0.0100	19.0832	19.0417	0.0415	87.8
1	2	-1	4.5223	4.5237	-0.0015	19.6141	19.6077	0.0065	38.9
2	1	1	4.3297	4.3357	-0.0060	20.4959	20.4672	0.0287	11.0
1	1	2	4.3000	4.3014	-0.0014	20.6387	20.6320	0.0066	31.1
2	1	-2	4.2406	4.2468	-0.0063	20.9312	20.9000	0.0312	24.7
1	2	1		4.2356	0.0050		20.9562	-0.0250	
3	0	-1	3.9702	3.9722	-0.0020	22.3745	22.3633	0.0112	15.4
2	2	0	3.8749	3.8720	0.0029	22.9321	22.9496	-0.0175	30.3
0	2	2	3.8401	3.8395	0.0007	23.1425	23.1467	-0.0042	36.5
2	0	2	3.6878	3.6858	0.0020	24.1127	24.1261	-0.0134	23.9
1	1	-3	3.6478	3.6519	-0.0041	24.3809	24.3533	0.0275	41.7
3	1	0		3.6417	0.0061		24.4222	-0.0414	
0	1	3	3.5822	3.5816	0.0006	24.8348	24.8388	-0.0040	31.7
2	1	2	3.4747	3.4722	0.0025	25.6157	25.6347	-0.0189	65.0
3	1	-2	3.4225	3.4244	-0.0019	26.0133	25.9982	0.0150	13.6
1	3	0	3.3074	3.3086	-0.0011	26.9349	26.9255	0.0094	30.3
0	3	1		3.3035	0.0040		26.9680	-0.0332	
3	1	1	3.2765	3.2732	0.0034	27.1938	27.2223	-0.0286	13.0
1	3	-1	3.2359	3.2353	0.0006	27.5423	27.5475	-0.0052	14.8
1	1	3		3.2341	0.0018		27.5578	-0.0155	
3	2	-1	3.1518	3.1510	0.0008	28.2920	28.2994	-0.0074	34.2
1	3	1	3.1282	3.1248	0.0034	28.5103	28.5417	-0.0314	10.1
1	2	-3	3.1169	3.1161	0.0009	28.6150	28.6232	-0.0082	40.6
2	2	2	3.0068	3.0022	0.0046	29.6871	29.7337	-0.0465	38.4
3	1	-3	2.9721	2.9737	-0.0016	30.0414	30.0251	0.0163	35.6
3	2	-2		2.9712	0.0010		30.0514	-0.0100	
2	3	0		2.9699	0.0022		30.0644	-0.0230	
3	0	2	2.9230	2.9211	0.0019	30.5580	30.5784	-0.0204	34.5
1	2	3	2.8457	2.8443	0.0014	31.4097	31.4260	-0.0163	32.3
2	3	1	2.7969	2.7965	0.0004	31.9725	31.9774	-0.0049	10.5
2	1	3		2.7957	0.0012		31.9864	-0.0139	
4	1	-2	2.776	2.7758	0.0002	32.2194	32.2220	-0.0026	19.6
3	2	-3	2.6633	2.6623	0.0010	33.6227	33.6358	-0.0131	38.8
3	3	-1	2.6061	2.6047	0.0014	34.3832	34.4016	-0.0184	29.9
0	4	0	2.5870	2.5876	-0.0005	34.6444	34.6371	0.0074	9.9
1	3	-3		2.5849	0.0021		34.6738	-0.0294	
1	1	4	2.5640	2.5614	0.0026	34.9651	35.0021	-0.0369	9.9
2	2	3	2.5341	2.5323	0.0018	35.3924	35.4183	-0.0258	21.6
3	3	-2	2.5017	2.5004	0.0013	35.8661	35.8853	-0.0192	30.3
1	4	-1	2.4940	2.4932	0.0009	35.9802	35.9930	-0.0128	29.9
3	0	3	2.4614	2.4572	0.0042	36.4731	36.5384	-0.0653	9.2
1	4	1	2.4466	2.4415	0.0051	36.7017	36.7809	-0.0792	31.3
1	3	3	2.4271	2.4233	0.0038	37.0072	37.0672	-0.0600	27.4
5	0	-1	2.3955	2.3976	-0.0021	37.5131	37.4795	0.0337	13.8
2	4	0	2.3676	2.3655	0.0021	37.9731	38.0080	-0.0349	34.0
2	4	-1	2.3584	2.3605	-0.0022	38.1270	38.0907	0.0363	36.8
5	0	-2		2.3594	-0.0010		38.1103	0.0167	
0	4	2		2.3580	0.0004		38.1332	-0.0062	
4	2	-3	2.3420	2.3430	-0.0010	38.4033	38.3869	0.0164	32.4
3	2	-4	2.3303	2.3303	-0.0001	38.6051	38.6038	0.0013	41.2
4	0	-4		2.3284	0.0018		38.6362	-0.0311	
3	3	-3	2.3091	2.3078	0.0013	38.9733	38.9959	-0.0226	19.1
5	1	0	2.2790	2.2771	0.0019	39.5087	39.5431	-0.0343	41.6

Continued

TABLE I. Continued

<i>h</i>	<i>k</i>	<i>l</i>	<i>d</i> <sub>obs</sub> (Å)	<i>d</i> <sub>cal</sub> (Å)	$\Delta d$	$2\theta_{\text{obs}}$ (°)	$2\theta_{\text{cal}}$ (°)	$\Delta 2\theta$	<i>I</i> / <i>I</i> <sub>o</sub>
2	4	1	2.2734	2.2750	-0.0016	39.6108	39.5816	0.0293	47.3
4	1	-4		2.2717	0.0017		39.6417	-0.0309	
0	1	5	2.2344	2.2364	-0.0020	40.3318	40.2946	0.0372	21.0
5	0	-3		2.2328	0.0015		40.3608	-0.0290	
3	0	-5	2.2082	2.2080	0.0002	40.8320	40.8351	-0.0031	27.2
0	3	4	2.1984	2.2032	0.0014	41.0210	40.9271	0.0939	26.3
5	1	-3	2.1829	2.1826	0.0002	41.3264	41.3312	-0.0048	29.9
5	2	-1	2.1734	2.1755	-0.0021	41.5155	41.4734	0.0421	33.0
3	1	-5	2.1594	2.1594	0.0000	41.7962	41.7964	-0.0002	13.3
5	2	-2	2.1475	2.1468	0.0007	42.0391	42.0538	-0.0147	9.6
4	2	-4	2.1237	2.1234	0.0003	42.5335	42.5389	-0.0054	30.4
1	1	5	2.1123	2.1106	0.0016	42.7742	42.8091	-0.0349	28.5
2	4	-3	2.1024	2.1002	0.0014	42.9844	43.0322	-0.0479	34.2
3	3	-4	2.0837	2.0814	0.0014	43.3898	43.4400	-0.0503	29.4
5	2	-3	2.0516	2.0502	0.0015	44.1042	44.1373	-0.0331	32.6
4	0	-5	2.0420	2.0442	0.0014	44.3223	44.2737	0.0486	31.5
3	2	-5	2.0263	2.0309	0.0014	44.6859	44.5787	0.1072	27.8
5	2	1	2.0169	2.0175	-0.0006	44.9040	44.8893	0.0147	29.1
5	1	-4		2.0158	0.0011		44.9303	-0.0263	
5	0	2	2.0064	2.0065	0.0000	45.1513	45.1510	0.0002	27.8
4	1	-5		2.0054	0.0010		45.1756	-0.0243	
3	3	3	1.9985	2.0015	0.0014	45.3403	45.2701	0.0702	28.1
1	2	5	1.9901	1.9902	-0.0001	45.5439	45.5416	0.0024	28.8
4	3	2	1.9640	1.9632	0.0008	46.1838	46.2030	-0.0191	26.5
2	0	-6	1.9506	1.9514	-0.0008	46.5183	46.4974	0.0209	8.4
2	5	0		1.9510	-0.0003		46.5097	0.0086	
6	1	-2		1.9505	0.0001		46.5214	-0.0031	
2	3	4		1.9504	0.0002		46.5228	-0.0045	
1	4	-4	1.9414	1.9428	-0.0014	46.7510	46.7163	0.0347	7.8
2	4	-4	1.9128	1.9132	-0.0003	47.4927	47.4841	0.0086	28.1
6	1	0		1.9118	0.0011		47.5207	-0.0279	
4	2	-5	1.9019	1.9012	0.0007	47.7836	47.8012	-0.0176	27.2
0	1	6	1.8761	1.8771	-0.0010	48.4816	48.4553	0.0264	30.6
5	3	-3		1.8745	0.0016		48.5253	-0.0437	
3	1	-6	1.8625	1.8634	-0.0009	48.8598	48.8350	0.0248	26.4
4	4	1		1.8628	-0.0003		48.8504	0.0093	
5	0	-5		1.8628	-0.0003		48.8518	0.0080	
6	2	-1		1.8614	0.0010		48.8889	-0.0292	
6	2	-2	1.8552	1.8542	0.0010	49.0634	49.0915	-0.0281	29.7
5	3	1	1.8485	1.8495	-0.0010	49.2524	49.2253	0.0272	27.9
1	4	4		1.8492	-0.0007		49.2336	0.0189	
6	0	1		1.8489	-0.0004		49.2410	0.0114	
4	0	4	1.8409	1.8429	0.0014	49.4706	49.4138	0.0568	27.2
5	1	-5	1.8333	1.8333	0.0000	49.6887	49.6893	-0.0006	31.5
2	2	-6	1.8258	1.8259	-0.0001	49.9069	49.9033	0.0036	30.6
6	1	1	1.8189	1.8201	-0.0012	50.1105	50.0737	0.0367	29.1
0	5	3		1.8197	-0.0009		50.0853	0.0252	
1	0	6		1.8183	0.0005		50.1265	-0.0160	
3	5	-2	1.7978	1.7981	-0.0003	50.7403	50.7311	0.0092	32.0
4	0	-6		1.7977	0.0001		50.7426	-0.0023	
4	3	3	1.7914	1.7922	-0.0008	50.9339	50.9093	0.0246	32.0
1	1	6		1.7909	0.0005		50.9485	-0.0147	
0	2	6		1.7908	0.0006		50.9518	-0.0180	
3	2	-6	1.7798	1.7789	0.0009	51.2898	51.3179	-0.0281	31.2
1	5	3	1.7680	1.7688	-0.0008	51.6582	51.6329	0.0253	28.6
4	4	2	1.7543	1.7546	-0.0003	52.0890	52.0795	0.0095	26.9
4	4	-4	1.7307	1.7308	-0.0002	52.8570	52.8506	0.0064	27.3
2	3	5	1.7182	1.7191	-0.0009	53.2691	53.2391	0.0301	25.5
6	3	0	1.6933	1.6945	-0.0012	54.1183	54.0762	0.0421	26.7
1	5	-4		1.6929	0.0004		54.1321	-0.0138	
2	5	3	1.6845	1.6856	-0.0011	54.4243	54.3856	0.0387	27.8
7	1	-1		1.6841	0.0004		54.4378	-0.0135	
2	0	-7	1.6775	1.6787	-0.0012	54.6678	54.6250	0.0428	26.4
5	0	-6		1.6787	-0.0011		54.6282	0.0396	
6	3	-3		1.6783	-0.0008		54.6405	0.0273	
0	5	4		1.6775	0.0000		54.6681	-0.0003	

Continued

TABLE I. Continued

<i>h</i>	<i>k</i>	<i>l</i>	<i>d</i> <sub>obs</sub> (Å)	<i>d</i> <sub>cal</sub> (Å)	$\Delta d$	$2\theta_{\text{obs}}$ (°)	$2\theta_{\text{cal}}$ (°)	$\Delta 2\theta$	<i>I</i> / <i>I</i> <sub>o</sub>
2	1	-7	1.6561	1.6571	-0.0010	55.4358	55.3997	0.0361	26.9
5	1	-6		1.6570	-0.0009		55.4028	0.0330	
1	4	5		1.6564	-0.0003		55.4261	0.0097	
5	0	4	1.6338	1.6346	-0.0008	56.2600	56.2290	0.0310	26.5
1	5	4	1.6303	1.6299	0.0004	56.3911	56.4074	-0.0162	26.5
6	3	1		1.6297	0.0006		56.4141	-0.0230	
4	4	3		1.6294	0.0009		56.4261	-0.0350	
7	0	-4	1.6121	1.6107	0.0014	57.0842	57.1384	-0.0542	24.6
5	3	3	1.6065	1.6060	0.0005	57.3028	57.3223	-0.0195	26.4
6	3	-4		1.6059	0.0006		57.3269	-0.0241	
2	2	-7	1.5958	1.5968	-0.0010	57.7211	57.6820	0.0391	25.3
5	2	-6		1.5968	-0.0009		57.6851	0.0360	
3	3	5		1.5967	-0.0008		57.6882	0.0329	
6	0	3	1.5911	1.5916	-0.0005	57.9084	57.8900	0.0184	25.5
7	1	-4		1.5916	-0.0004		57.8908	0.0176	
4	0	-7		1.5915	-0.0004		57.8931	0.0153	
5	4	2	1.5849	1.5856	-0.0007	58.1582	58.1290	0.0292	24.8
1	6	-3	1.5782	1.5778	0.0004	58.4267	58.4443	-0.0177	24.4
5	5	0	1.5479	1.5488	-0.0009	59.6880	59.6488	0.0392	26.7
4	5	-4		1.5471	0.0008		59.7216	-0.0336	
6	3	2	1.5433	1.5430	0.0003	59.8815	59.8962	-0.0147	28.4
3	6	1		1.5429	0.0004		59.8977	-0.0162	
6	4	-3		1.5424	0.0010		59.9228	-0.0413	
0	4	6	1.5360	1.536	0.0000	60.1959	60.1950	0.0010	26.3
0	5	5		1.5358	0.0002		60.2060	-0.0101	
6	1	-6		1.5351	0.0009		60.2341	-0.0382	
5	4	-5	1.5115	1.5118	-0.0002	61.2748	61.2637	0.0110	25.1
0	7	0	1.4778	1.4786	-0.0008	62.8303	62.7915	0.0388	25.7
3	4	5		1.4783	-0.0005		62.8071	0.0232	
0	3	7		1.4783	-0.0005		62.8084	0.0219	
0	6	4		1.4776	0.0002		62.8407	-0.0104	
5	3	4		1.4772	0.0006		62.8589	-0.0287	
1	0	-8	1.4617	1.4621	-0.0004	63.6045	63.5852	0.0194	24.7
5	5	-4	1.4579	1.4585	-0.0006	63.7898	63.7608	0.0290	24.7
4	5	-5	1.4541	1.4545	-0.0004	63.9750	63.9542	0.0208	24.3
4	6	-3	1.4432	1.4421	0.0014	64.5181	64.5722	-0.0541	24.3
4	1	6	1.4379	1.4377	0.0001	64.7833	64.7907	-0.0074	24.4
8	2	0	1.4041	1.4042	-0.0002	66.5435	66.5353	0.0081	23.4
0	5	6		1.4032	0.0008		66.5869	-0.0435	
5	7	0	1.2487	1.2491	-0.0004	76.1776	76.1458	0.0319	22.0
2	8	1		1.2488	-0.0001		76.171	0.0066	
4	7	-4		1.2482	0.0005		76.2105	-0.0328	

The *d*-values were calculated using CuK $\alpha$ <sub>1</sub> radiation ( $\lambda = 1.5405981$  Å).

graphical interface (Blanton et al., 2019) with figures of merit:  $M(20) = 16.8$  and  $F(20) = 40.0$  (0.0132, 38). Analysis of the systematic absences using EXPO2013 (Altomare et al., 2013) suggested the space group  $P2_1/n$  (No. 14) (Table I). The refinement was performed with TOPAS v.6 (Pawley, 1981) fitting using the whole powder pattern decomposition (WPPD) procedure. A Chebyshev Polynomial was used to fit the background (Figure 2). The final Pawley fit yielded the unit-cell parameters  $a = 12.0225(8)$  Å,  $b = 10.3812(9)$  Å,  $c = 11.7823(9)$  Å,  $\beta = 103.180(9)^\circ$ , unit-cell volume  $V = 1431.79$  Å<sup>3</sup>, and  $Z = 4$  (Table II). The lack of impurity lines and good residual values from Pawley fit ( $R_{\text{exp}}$ ,  $R_{\text{wp}}$ ,  $R_{\text{p}}$ , and GoF) obtained from the refinement process allowed to conclude that the sample corresponds to a single-phase and high-quality experimental data was obtained. The volumetric thermal expansion coefficient ( $\alpha = 5.78 \times 10^{-5}$  K<sup>-1</sup>) has been determined using the unit-cell volume obtained in this study at 298 K and the value reported per single crystal at 100 K, using the following relation:  $\ln(V/V_o) = \alpha(T - T_o)$

TABLE II. Experimental data for dichloro-dioxido-(4,4'-dimethyl-2,2'-bipyridyl)-molybdenum (VI) complex using powder and single crystal analysis.

Methodology	Powder analysis	Single crystal analysis <sup>a</sup>
Empirical formula	C <sub>12</sub> H <sub>12</sub> Cl <sub>2</sub> MoN <sub>2</sub> O <sub>2</sub>	C <sub>12</sub> H <sub>12</sub> Cl <sub>2</sub> MoN <sub>2</sub> O <sub>2</sub>
Formula weight	383.1	383.1
Crystal system	Monoclinic	Monoclinic
Space group	$P2_1/n$ (No. 14)	$P2_1/n$ (No. 14)
<i>a</i> (Å)	12.0225 (8)	11.956 (2)
<i>b</i> (Å)	10.3812 (9)	10.369 (2)
<i>c</i> (Å)	11.7823 (9)	11.746 (2)
$\alpha$ (°)	90	90
$\beta$ (°)	103.180 (9)	103.57 (2)
$\gamma$ (°)	90	90
Volume (Å <sup>3</sup> )	1431.79 (2)	1415.5 (5)
<i>Z</i>	4	—
$R_{\text{exp}}$	1.05	—
$R_{\text{wp}}$	3.76	—
$R_{\text{p}}$	2.12	—
GoF	3.57	—

<sup>a</sup>Baird et al. (1996).

(Megaw, 1971; Ishige et al., 2017; van der Lee and Dumitrescu, 2021).

## ACKNOWLEDGEMENTS

This work was financially supported by the Universidad Nacional de Colombia and the Facultad de Ciencias de la Universidad Nacional de Colombia by the internal Projects code Hermes 52711. N.J.C. appreciates the collaboration of the Professor Luis Carlos Moreno from the X-Ray Powder Diffraction laboratory of Universidad Nacional de Colombia.

## CONFLICTS OF INTEREST

The authors have no conflicts of interest to declare.

## REFERENCES

- Altomare, A., C. Cuocci, C. Giacomazzo, A. Moliterni, R. Rizzi, N. Corriero, and A. Falcicchio. 2013. "EXPO2013: A Kit of Tools for Phasing Crystal Structures from Powder Data." *Journal of Applied Crystallography* 46 (4): 1231–5. doi:10.1107/S0021889813013113.
- Baird, D. M., F. L. Yang, D. J. Kavanaugh, G. Finness, and K. R. Dunbar. 1996. "Ligand Effects on the  $\delta \rightarrow \delta^*$  Band Energies and Intensities in a Series of Diimine Complexes of Dimolybdenum." *Polyhedron* 15 (15): 2597–606. doi:10.1016/0277-5387(95)00535-8.
- Bakhtchadjian, R., S. Tsarukyan, J. Barrault, F. Martinez, L. Tavadyan, and N. J. Castellanos. 2011. "Application of a Dioxo-Molybdenum(VI) Complex Anchored on TiO<sub>2</sub> for the Photochemical Oxidative Decomposition of 1-Chloro-4-Ethylbenzene Under O<sub>2</sub>." *Transition Metal Chemistry* 36 (8): 897–900. doi:10.1007/s11243-011-9547-2.
- Blanton, J. R., R. J. Papoular, and D. Louër. 2019. "PreDICT: A Graphical User Interface to the DICVOL14 Indexing Software Program for Powder Diffraction Data." *Powder Diffraction* 34 (3): 233–41. doi:10.1017/S0885715619000514.
- Boultif, A., and D. Louër. 2004. "Powder Pattern Indexing with the Dichotomy Method." *Journal of Applied Crystallography* 37 (5): 724–31. doi:10.1107/S0021889804014876.
- Castellanos, N. J. 2014. Molecular Oxygen Activation by Oxo-Molybdenum as a Heterogeneous Catalytic System in *Molybdenum and Its Compounds: Applications, Electrochemical Properties and Geological Implications* (pp. 87–106). <https://novapublishers.com/shop/molybdenum-and-itscompounds-applications-electrochemical-properties-andgeological-implications/>.
- Castellanos, N. J., F. Martínez, E. A. Páez-Mozo, F. Ziarelli, and H. Arzoumanian. 2012. "Bis(3,5-Dimethylpyrazol-1-yl)Acetate Bound to Titania and Complexed to Molybdenum Dioxide as a Bidentate N, N'-Ligand. Direct Comparison with a Bipyridyl Analog in a Photocatalytic Arylalkane Oxidation by O<sub>2</sub>." *Transition Metal Chemistry* 37 (7): 629–37. doi:10.1007/s11243-012-9631-2.
- Castellanos, N. J., F. Martínez, F. Lynen, S. Biswas, P. Van Der Voort, and H. Arzoumanian. 2013. "Dioxygen Activation in Photooxidation of Diphenylmethane by a Dioxomolybdenum(VI) Complex Anchored Covalently onto Mesoporous Titania." *Transition Metal Chemistry* 38 (2): 119–27. doi:10.1007/s11243-012-9668-2.
- Castellanos, N. J., H. Martínez, F. Martínez, K. Leus, and P. Van Der Voort. 2021. "Photo-Epoxidation of ( $\alpha$ ,  $\beta$ )-Pinene with Molecular O<sub>2</sub> Catalyzed by a Dioxo-Molybdenum (VI)-based metal-organic framework." *Research on Chemical Intermediates* 47 (10): 4227–44. doi:10.1007/s11164-021-04518-3.
- Dupé, A., M. E. Judmaier, F. Belaj, K. Zangger, and N. C. Möscher-Zanetti. 2015. "Activation of Molecular Oxygen by a Molybdenum Complex for Catalytic Oxidation." *Dalton Transactions* 44 (47): 20514–22. doi:10.1039/c5dt02931g.
- Heinze, K. 2015. "Bioinspired Functional Analogs of the Active Site of Molybdenum Enzymes: Intermediates and Mechanisms." *Coordination Chemistry Reviews* 300: 121–41. doi:10.1016/j.ccr.2015.04.010.
- Hille, R., T. Nishino, and F. Bittner. 2011. "Molybdenum Enzymes in Higher Organisms." *Coordination Chemistry Reviews* 255 (9–10): 1179–205. doi:10.1016/j.ccr.2010.11.034.
- Ishige, R., T. Masuda, Y. Kozaki, E. Fujiwara, T. Okada, and S. Ando. 2017. "Precise Analysis of Thermal Volume Expansion of Crystal Lattice for Fully Aromatic Crystalline Polyimides by X-ray Diffraction Method: Relationship between Molecular Structure and Linear/Volumetric Thermal Expansion." *Macromolecules* 50 (5): 2112–23. doi:10.1021/acs.macromol.7b00095.
- Kapp, R. W. 2014. Molybdenum in *Encyclopedia of Toxicology: Third Edition* (pp. 383–388). Academic Press. doi:10.1016/B978-0-12-386454-3.00884-8.
- Kück, J. W., R. M. Reich, and F. E. Kühn. 2016. "Molecular Epoxidation Reactions Catalyzed by Rhenium, Molybdenum, and Iron Complexes." *Chemical Record* 16 (1): 349–64. doi:10.1002/tcr.201500233.
- Martínez, H., Á. A. Amaya, E. A. Páez-Mozo, and F. Martínez. 2018. "Highly Efficient Epoxidation of Alfa-Pinene with O<sub>2</sub> Photocatalyzed by Dioxo Mo<sup>(VI)</sup> Complex Anchored on TiO<sub>2</sub> Nanotubes." *Microporous and Mesoporous Materials* 265 (November 2017): 202–10. doi:10.1016/j.micromeso.2018.02.005.
- Martínez, H., Á. A. Amaya, E. A. Páez-Mozo, F. Martínez, and S. Valange. 2020. "Photo-Assisted O-Atom Transfer to Monoterpenes with Molecular Oxygen and a DioxoMo<sup>(VI)</sup> Complex Immobilized on TiO<sub>2</sub> Nanotubes." *Catalysis Today* (June). doi:10.1016/j.cattod.2020.07.053.
- Martínez, H., E. A. Páez-Mozo, and F. Martínez. 2021. "Selective Photo-epoxidation of (R)-(+)- and (S)-(-)-Limonene by Chiral and Non-Chiral Dioxo-Mo<sup>(VI)</sup> Complexes Anchored on TiO<sub>2</sub>-Nanotubes." *Topics in Catalysis* 64 (1–2): 36–50. doi:10.1007/s11244-020-01355-3.
- Martínez, H., D. F. Valezi, E. Di Mauro, E. A. Páez-Mozo, and F. Martínez. 2022. "Characterization of Peroxo-Mo and Superoxo-Mo Intermediate Adducts in Photo-Oxygen Atom Transfer with O<sub>2</sub>." *Catalysis Today* (February 2021). doi:10.1016/j.cattod.2022.02.016.
- Megaw, H. D. 1971. "Crystal Structures and Thermal Expansion." *Materials Research Bulletin* 6 (10): 1007–18. doi:10.1016/0025-5408(71)90080-8.
- Pawley, G. S. 1981. "Unit-Cell Refinement from Powder Diffraction Scans." *Journal of Applied Crystallography* 14 (6): 357–61. doi:10.1107/s0021889881009618.
- Schoepp-Cothenet, B., R. Van Lis, P. Philippot, A. Magalon, M. J. Russell, and W. Nitschke. 2012. "The Ineluctable Requirement for the Trans-Iron Elements Molybdenum and/or Tungsten in the Origin of Life." *Scientific Reports* 2 (1): 1–5. doi:10.1038/srep00263.
- van der Lee, A., and D. G. Dumitrescu. 2021. "Thermal Expansion Properties of Organic Crystals: A CSD Study." *Chemical Science* 12 (24): 8537–47. doi:10.1039/d1sc01076j.